A Silylene Stabilized by a σ-Donating Nickel(0) Fragment

María Frutos, Nasrina Parvin, Antoine Baceiredo, David Madec, Nathalie Saffon-merceron, Vicenç Branchadell, Tsuyoshi Kato

Coordination Chemistry Hot Paper

How to cite: *Angew. Chem. Int. Ed.* **2022,** *61,* e202201932
International Edition: doi.org/10.1002/anie.202201932
German Edition: doi.org/10.1002/ange.202201932

A Silylene Stabilized by a σ-Donating Nickel(0) Fragment

*María Frutos, Nasrina Parvin, Antoine Baceiredo, David Madec, Nathalie Saffon-Merceron, Vicenç Branchadell, and Tsuyoshi Kato**

Abstract: A donor-stabilized silylene **4** featuring a Ni^0-based donating ligand was synthesized. Complex **4** exhibits a pyramidalized and nucleophilic Si^{II} center and shows a peculiar behavior due to the cooperative reactivity of Si and Ni centers. Calculations indicate that the orientation of Ni-ligands with respect to the silylene moiety is crucial in determining the role of the Ni-fragment (Lewis acid or Lewis base) towards silylene. Indeed, a simple 90° rotation of the Si–Ni bond, reverses the role of Ni, and transforms a classical silylene→Ni^0 complex into an unprecedented Ni^0→silylene complex.

Transition metals basically act as Lewis acids and thus form various complexes **I** interacting with Lewis base ligands (Figure 1). Despite less common, transition metals also act as Lewis bases[1] to interact with Lewis acids (A) to form non-classical M→A complexes **II**. This non-classical mode of interaction (known as Z-ligands[2] or metal-only Lewis pairs[3]) leads to new methods to tune/improve properties of transition metals.[4] Singlet divalent group-14 species **III** such as carbenes and their heavier analogues (R_2E, E=C, Si, Ge…), featuring a divalent E center with a lone pair orbital (n_σ) and a vacant orbital (p_π), present an ambiphilic character. Consequently, like in the case of transition metals, there are potentially two coordination modes via σ-electron donation: i) either from R_2E to metal [R_2E:→M] **IV** or, ii) from metal to ER_2 [M→ER_2] **V**. Classical $R_2E^{\bullet}$→M complexes **IV**, presenting a planar E atom, categorized as Fischer- or Schrock-types complexes,[5] are ubiquitous and play an important role in synthetic chemistry. In contrast, and not surprisingly, M→ER_2 complexes **V**, characterized by a strongly pyramidalized E center as base-stabilized metallylene **VI**, are less common and only a few examples are known. How could the formation of such non-classical complexes **V** be promoted? On descending a group in the periodic table, the nucleophilicity of divalent atom (E) decreases (increasing s-character of lone pair) and the unoccupied p_π orbital becomes more Lewis acidic. Therefore, heavier divalent species (E=Ge, Sn, Pb) present stronger tendency to form M→ER_2 complexes **V**. Indeed, to date, the only known compounds of this type **V** are germylene-, stannylene- and plumbylene-based complexes (**VII**–**X**).[6–9] DFT calculations predicted that, although germylenes and stannylenes are able to form complexes of type **V**, lighter analogues (silylenes and carbenes) tend to form classical R_2E:→M complexes **IV**,[7] although several methanediide-TM complex, featuring a pyramidalized carbon centre, have been described.[10] To the best of our knowledge, complexes **V** involving a silylene fragment M→SiR_2 remain elusive, and no clear synthetic access has been proposed, despite their potential usefulness as an extended model of Lewis base-stabilized silylenes **VI**.

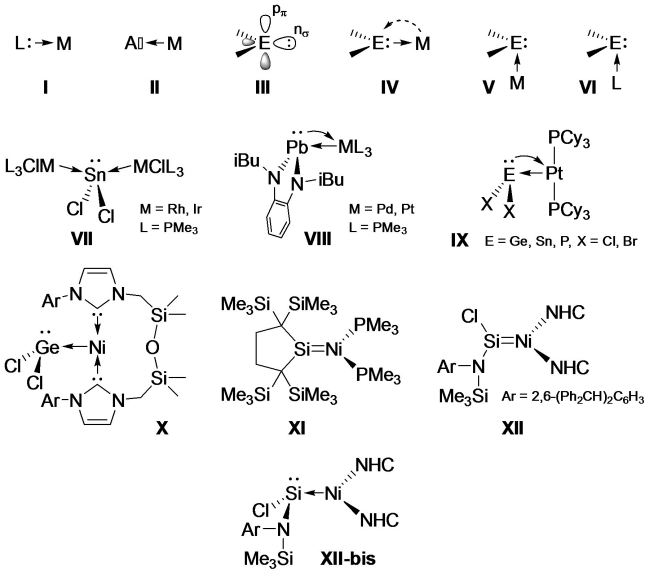

Figure 1. Classical and non-classical metallylene complexes.

[*] Dr. M. Frutos, Dr. N. Parvin, Dr. A. Baceiredo, Dr. D. Madec, Dr. T. Kato
Laboratoire Hétérochimie Fondamentale et Appliquée (UMR 5069), Université de Toulouse, CNRS
118 route de Narbonne, F-31062 Toulouse (France)
E-mail: tsuyoshi.kato@univ-tlse3.fr
Homepage: https://lhfa.cnrs.fr/

Dr. N. Saffon-Merceron
Institut de Chimie de Toulouse (UAR 2599), Université de Toulouse, CNRS
118 route de Narbonne, F-31062 Toulouse (France)

Prof. V. Branchadell
Departament de Química,
Universitat Autònoma de Barcelona
08193 Bellaterra (Spain)

Here, we would like to report the synthesis of an unusual 16e-nickel(0)-silylene complex **4**, presenting a strongly pyramidalized and nucleophilic divalent silicon center, which can be regarded as a silylene complex stabilized by coordination of σ-donating Ni^0 ligand. DFT calculations indicate that the orientation of Ni-ligands relative to silylene fragment is crucial in determining the coordination mode of $R_2Si\text{-}Ni^0L_2$ complexes, and a simple 90° rotation of Si–Ni bond reverses the role of Ni-fragment which turns from Lewis acid to Lewis base (**IV**→**V**).

16e-Ni^0 complexes featuring silylene ligands (**XI**, **XII**) usually present a short Si=Ni double bond and two trigonal planar Si and Ni centers which are perpendicular to each other.[11] We have computationally studied Ni^0-silylene complexes by hypothesizing that the Si=Ni π-bond can be broken through a rotational distortion around SiNi-bond axis and thus changing the coordination mode. Calculations predict that such a 90° SiNi-bond rotation in complex model $H_2Si{=}Ni(PMe_3)_2$ **1**, affording rotamer **2**, is only moderately exergonic ($\Delta G_{\mathbf{1}\rightarrow\mathbf{2}} = 6.6$ kcal mol^{-1}) and leads to a dramatic geometrical modification (Figure 2). Indeed, rotamer **2** exhibits a strongly pyramidalized Si center ($\Sigma^\circ_{Si} = 305.9°$) and a considerably elongated Si–Ni bond (2.249 Å) compared to that of **1** (2.118 Å). This structural feature of **2** is in agreement with a Si atom holding a lone pair of electrons and a reduced Si–Ni multiple bonding character. Indeed, it was found that the negative charge of H_2Si fragment in **2** [−0.40 (H_2Si)/+0.40 ($Ni(PMe_3)_2$)] is increased from that in **1** [−0.17 (H_2Si)/+0.17 ($Ni(PMe_3)_2$)] and that the Wiberg and Mayer bond orders of the Si–Ni bond of **2** (0.602 and 0.812) are smaller than those calculated for **1** (0.820 and 1.163). Furthermore, intrinsic bond orbital (IBO) analysis[12] of **1** clearly indicates the presence of a Si=Ni double bond constituted of $R_2Si{:}\rightarrow$Ni σ-donation (Si–Ni σ-bonding orbital with a main occupancy at Si, Figure 2a) and π-back donation from Ni to Si (π-bonding orbital with a main occupancy at Ni, Figure 2b). In marked contrast, in the case of rotamer **2**, a large part of Si–Ni σ-bonding electrons is localized at the Ni atom (0.38 at Si and 1.60 at Ni, Figure 2c), in agreement with a Ni→Si σ-donation. Furthermore, the IBO analysis also indicates the presence of a lone pair localized on the Si atom in **2** with no contribution at Ni (1.90 at Si and 0.00 at Ni, Figure 2d), instead of π-bonding orbital. These results demonstrate that a 90° rotation of Si–Ni bond in **1** induces, not only the SiNi-π-bond breaking but also the reversal of the role of Ni^0-fragment: from Lewis acid (coordination center) to Lewis base (coordinating ligand).

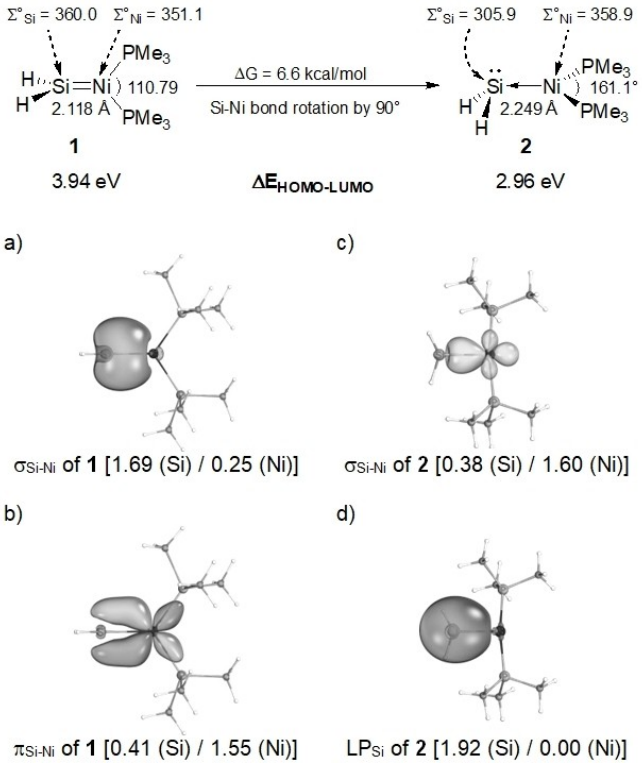

Figure 2. Calculated free energy ΔG (kcal mol^{-1}) for the isomerization of silylene-Ni^0 complex **1** to the corresponding rotamer **2** by a 90° rotation of Si–Ni bond as well as the geometry and selected intrinsic bond orbitals (IBOs) of each rotamer (**1** and **2**). Values in parenthesis are the contributions of Si–Ni σ- and π-bonding electrons at Si and Ni atoms.

Driess' complex **XII**[11b] undergoes a similar isomerization with a relatively small energy ($\Delta G_{\mathbf{XII}\rightarrow\mathbf{XII\text{-}bis}} =$ 12.1 kcal mol^{-1}) affording rotamer **XII-bis** (Figure 1) with a strongly pyramidalized Si center ($\Sigma^\circ_{Si} = 337.73°$) and a single Si–Ni bond (2.244 Å). Of particular interest, such geometrical and electronic modifications of silylene-nickel complexes (**1**→**2** and **XII**→**XII-bis**) induce a considerable decrease of HOMO–LUMO energy gaps ($\Delta E_{\text{HOMO-LUMO}}$: 3.49 eV for **1** vs 2.96 eV for **2** and 4.19 eV for **XII** vs 2.73 eV for **XII-bis**), and therefore an increased reactivity of the non-classical complexes (type **V**) compared to classical ones (type **IV**). In contrast, in the case of the corresponding carbene complexes [$R_2C{-}Ni(PMe_3)_2$, R=H, F], such a geometrical change was not observed by the C–Ni bond rotation and the classical carbene→Ni complex (with a planar carbon center and a short C=Ni double bond) was calculated to be the only stable isomer.

In order to verify the theoretical results, we have considered the use of a rigid planar bridging system connecting silylene- and metal-fragments which imposes such a bond rotated geometry of silylene-Ni complex of non-classical complexes of type **V**. For this purpose, we employed the phosphine-stabilized (amino)(chloro)silylene **3**[13] as a precursor, in which the amino substituent and the phosphine ligand are linked by a planar olefin bridge. Similarly to the synthesis of complex **XII**,[11b] the two successive additions of equimolar amounts of $Ni(COD)_2$, and N-heterocyclic carbene (NHC), to chlorosilylene **3**, in fluorobenzene at RT, afford silylene-Ni^0 complex **4** (Scheme 1). The reaction probably proceeds via the insertion of Ni into the Si^{II}–P bond followed by the COD ligand substitution by NHC at the Ni center. Complex **4** was isolated as air-sensitive crystals from a THF solution at RT (yield 70 %).

Even though silylene complex **4** slowly decomposes in solution (THF, fluorobenzene) ($t_{1/2} = 2$ days at RT, and $t_{1/2} =$ 2 h, at 80 °C), it was characterized by NMR spectroscopy. In the ^{29}Si NMR spectrum, a doublet signal appears at

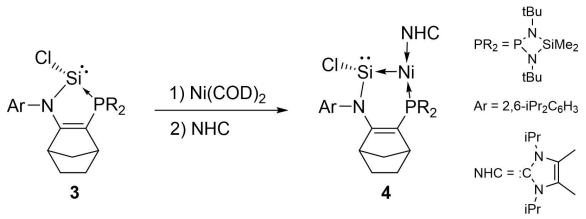

Scheme 1. Synthesis of Ni-stabilized silylene **4**.

138.1 ppm ($^2J_{SiP}$ = 71.8 Hz) in the region of that of the related acyclic (chloro)aminosilylene-Ni^0 complex **XII** (δ = 123.2 ppm)[11b] but significantly downfield compared to the starting phosphine-stabilized silylene **3** (−10.5 ppm).[13] The ^{31}P NMR spectrum displays a singlet signal at 91.4 ppm, also downfield shifted compared to **3** (75.0 ppm). A doublet signal observed at 186.7 ppm in ^{13}C NMR spectrum was attributed to the divalent carbon of NHC ligand. The relatively large carbon–phosphorus coupling constant ($^2J_{CP}$ = 50.4 Hz) is in good agreement with the T-shaped geometry around the Ni atom with the NHC ligand in a *trans*-position relative to the phosphine.[8c]

The molecular structure of **4**[14] reveals a strongly pyramidalized Si1 center (Σ°_{Si} = 321.58°) similarly to the case of the phosphine-stabilized silylene **3** (Σ°_{Si} = 292.0)[13] and an elongated Si–Ni bond (2.178 Å) compared to other Ni^0-silylene complexes (2.075 - 2.133 Å) (Figure 3).[10] This value is within the range of Ni–Si single bonds.[15] These structural data of **4** are in agreement with a non-classical complex **V** (Ni→silylene) with a lone pair on the Si atom and a reduced Si–Ni multiple bonding character. The Ni^0 site presents a planar and T-shaped geometry (Σ°_{Ni} = 359.91) with a large P–Ni–C1$_{NHC}$ angle (164.51°), in contrast to the case of silylene-Ni(NHC)$_2$ complex **XII** with a trigonal planar Ni site (C$_{NHC}$–Ni–C$_{NHC}$ = 111.4°).[11] A similar geometry was observed for other M^0→metallylene complexes **IX**–**X** (M=Ni, Pt)[8,9] as well as for L$_2$Ni→Lewis acid complexes.[16]

To gain more insight into the electronic structure of Ni^0→silylene complex **4**, DFT calculations have been performed at the M06/Def2TZVP//M06/6-31G(d) level of theory (Figure 4). The optimized structure of **4** agrees quite well with the experimentally observed one (Si–Ni: 2.227 Å, Si–N: 1.831 Å, Si–Cl: 2.19 Å, C1–Ni–P: 169.47°, Σ°_{Si} = 319.37°). The highest occupied molecular orbital (HOMO, −4.418 eV) corresponds to the lone pair orbital mainly localized on the Si atom and the lowest unoccupied bond orbital (LUMO, −1.389 eV) corresponds to the anti-bonding σ*-orbital of Si–Ni bond with a large coefficient on the Ni atom. Similar to the case of **XII-bis**, the HOMO–LUMO energy gap of **4** ($\Delta E_{HOMO\text{-}LUMO}$: 3.03 eV) is calculated to be small, suggesting an enhanced reactivity. As expected, IBO analysis of **4** show the same pattern of Ni→Si σ-bond and Si-lone pair (n$_{Si}$) orbitals as those calculated for **2** (Figure 1c, d) (see the Supporting Information).

In agreement with the MO analysis, contrary to other silylene-Ni complexes presenting an electrophilic character at the Si atom,[11a,17] silylene complex **4** presents a nucleophilic Si center, which has been demonstrated by the immediate reaction with MeOTf, leading to Si-methylated Ni^{II} complex **5** (Scheme 2). In contrast, a Lewis base such as *iso*-propyl isocyanide coordinates on the metal center to form a tetra-coordinate Ni^0 complex **6**. A less pyramidalized Si^{II} center (Σ°_{Si} = 349.69°) and a shorten Si–Ni bond [2.1108

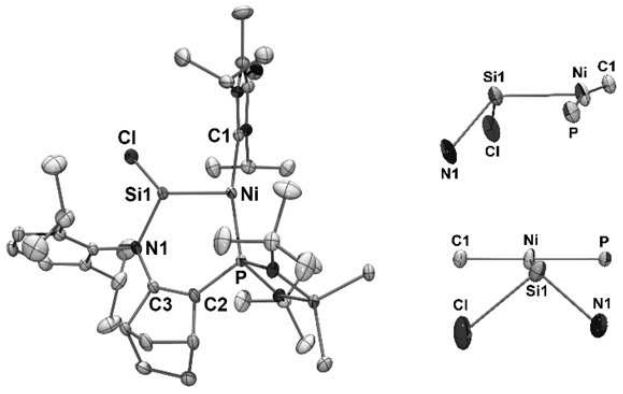

Figure 3. Molecular structures of **4**. Thermal ellipsoids represent 30% probability. H and disordered atoms are omitted for clarity. Selected bond lengths [Å] and angles [°]: Si1–Ni 2.178(1), N1–Si1 1.840(2), Si1–Cl 2.196(1), Ni–C1 1.934(2), Ni–P 2.126(1), P–C2 1.762(2), C2–C3 1.359(3), C3–N1 1.360(2); Cl–Si1–N1 95.35(6), Cl–Si1–Ni 110.94(4), N1–Si1–Ni 115.29(6), Si1–Ni–C1 101.53(6), C1–Ni–P 164.51(6), Si1–Ni–P 93.87(2), Ni–P–C2 117.05(7), P–C2–C3 129.90(16), C2–C3–N1 129.62(18), C3–N1–Si1 117.17(13). Σ°_{Si} = 321.58°. Torsion angles: C1–Ni-Si1–Cl = 33.16(7)°, P–Ni–Si1–N1 = 38.21(7)°.

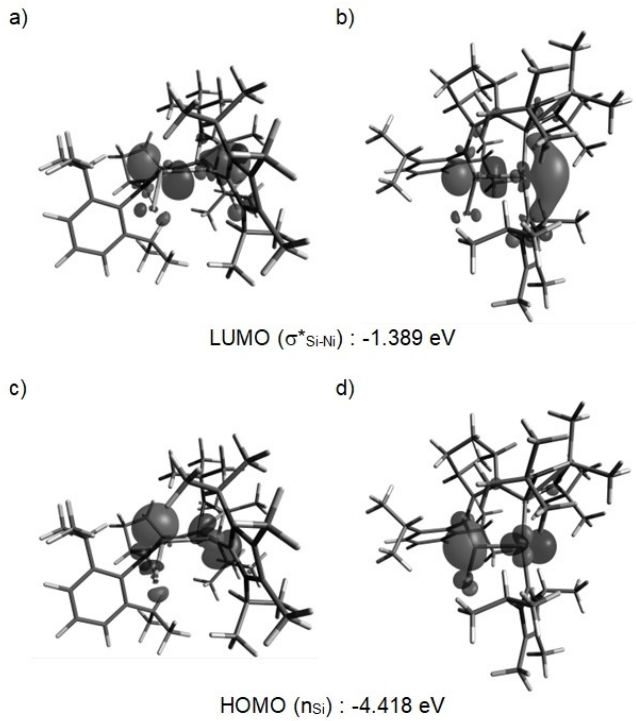

Figure 4. Frontier molecular orbitals [LUMO (a, b) and HOMO (c, d)] of **4** (isosurface level = ±0.05 e/(a.u.)^3) and their energy levels (eV) calculated at the M06/Def2TZVP level.

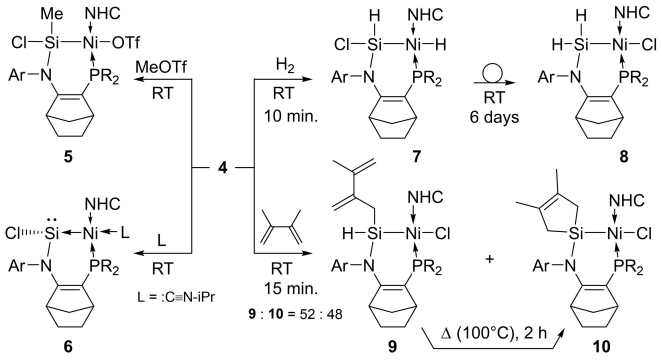

Scheme 2. Reactions of Ni-stabilized chlorosilylene complex **4**.

(5) Å] in **6** compared to those of **4** [$\Sigma°_{Si}$ = 321.58°, Si–Ni: 2.1780(7) Å] suggest an enhanced Si→Ni π-back donation in **6** probably due to the geometrical modification at Ni^0 center (T-shape→distorted tetrahedral).

Silylene complex **4** also readily reacts with H_2 at RT to afford a formal 1,2-dihydrogen adduct **7** which slowly isomerizes to the corresponding isomer **8** by the substituent exchange of H and Cl on the Si and Ni atoms respectively (Scheme 2 and Figure 5). Although intermediate **7** could not be isolated, the two ^{1}H NMR signals corresponding to the Si–H (4.92 ppm, J_{HH} = 6.5 Hz, J_{PH} = 5.6 Hz, J_{SiH} = 176.5 Hz) and Ni–H (−6.49 ppm, J_{HH} = 6.5 Hz, J_{PH} = 56.5 Hz, J_{SiH} = 86.0 Hz) appearing in the characteristic regions indicate its formation. Typically, the large *trans* coupling-constants ($^2J_{Si–H}$ = 86.0 Hz, $^2J_{P–C(NHC)}$ = 82.8 Hz) suggest a square-planar geometry around the Ni^{II} atom in **7** with the Ni–H function at the *trans*-position relative to the Si atom. The structure of dihydrosilane-Ni^{II} complex **8** was confirmed by X-ray diffraction analysis.[14]

Silylene-Ni **4** complex also readily reacts with 2,3-dimethyl-1,3-butadiene at RT to give a mixture of two Si^{VI}-Ni^{II} complexes (**9** and **10**) with a 1:1 ratio, which are formally formed by either a C–H insertion or a [4+1] cycloaddition at the Si center followed by a 1,2-migration of chlorine atom to the Ni center, respectively (Scheme 2). Of particular interest, complex **9** isomerizes at 100 °C to give cycloadduct **10** in 2 h. Calculations predict that both reactions start with a formal 1,2-addition of butadiene to the Si–Ni moiety, either via an ene-type reaction of the allylic C–H group, or by a [4+2]-cycloaddition reaction, followed by the isomerization of the resulting intermediates via 1,2-migrations of the ligands onto the Si and Ni atoms to give the experimentally obtained **9** and **10** (see Supporting Information). In both cases, the first step is the most costly step (1,2-addition or [4+2]-cycloaddition), with very similar energy barriers ($\Delta G^{\ddagger}$ = 21.3 and 20.7 kcal mol^{-1}, respectively), which is consistent with the formation of **9** and **10** in the same proportions. Calculations also indicate that the isomerization of **9** to **10** proceeds via a tautomerization of **9** to generate a zwitterionic intermediate **12** that cyclizes to give **10** (Figure 6). The experimental thermal activation required for this isomerization (100 °C) is in agreement with a considerably high energy barrier ($\Delta G^{\ddagger}_{9\rightarrow12}$ = 37.9 kcal mol^{-1}) and the endergonic nature of the tautomerization step ($\Delta G_{9\rightarrow12}$ = 30.3 kcal mol^{-1}).

In order to check the substituent effect on the reactivity/stability of the Ni→Si complexes, we have also tested the substitution of chloride on the Si atom in **4** by PhLi. The reaction of **4** with PhLi (1 equiv) proceeds smoothly at −80 °C to generate the corresponding phenyl-substituted silylene complex **13** (Scheme 3). The formation of **13** was indicated by the characteristic ^{29}Si NMR chemical shift for the Si^{II} atom (δ = 154.2 ppm, J_{SiP} = 85.6 Hz). However, phenylsilylene complex **13** is less stable than its precursor **4**

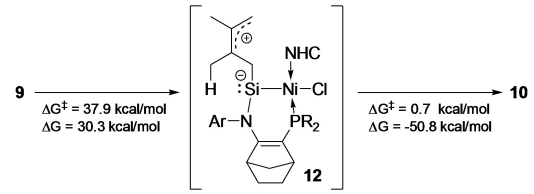

Figure 6. Calculated reaction pathway for the isomerization of **9** to **10**.

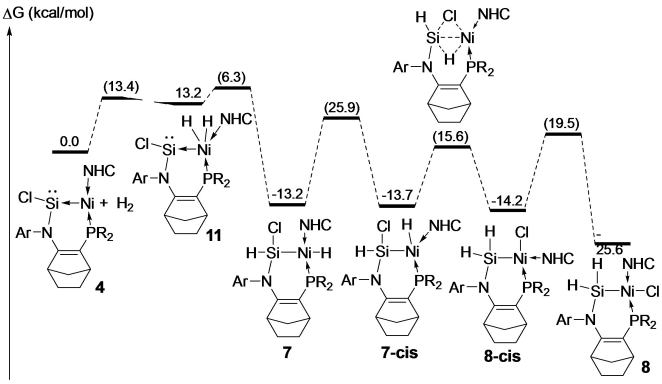

Figure 5. Calculated reaction pathways for the hydrogenation of **4** and calculated relative Gibbs energies Δ*G* (kcal mol^{-1}) of each intermediate and product **8** from that of **4** + H_2. In parenthesis are calculated Gibbs energy barriers $\Delta G^{\ddagger}$ (kcal mol^{-1}).

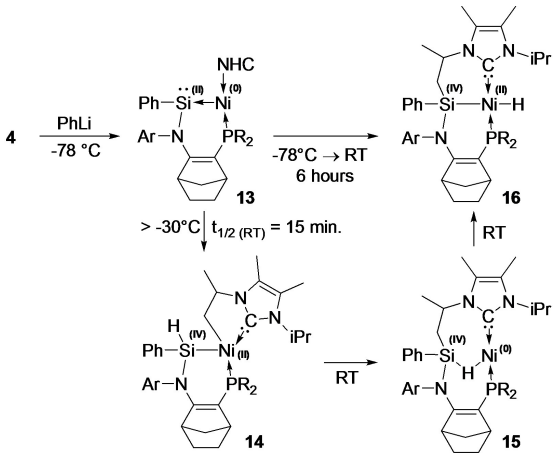

Scheme 3. Synthesis of phenyl-substituted silylene **13** and its isomerization.

and starts evolving above −30 °C via a 1,2-addition of the C–H moiety of NHC ligand across the Si–Ni fragment to give the silyl hydride Si^{IV}-Ni^{II} complex **14** (isomerization completed within 30 min at RT). The formation of **14** is supported by the characteristic signals observed for the Si–H group in the ^{1}H NMR spectrum ($\delta = 5.36$ ppm, $^3J_{HP} = 5.2$ Hz, $^1J_{SiH} = 153.1$ Hz) and for the CH_2-Ni moiety in the ^{13}C NMR spectrum ($\delta = 45.0$ ppm, $^2J_{CP} = 12.8$ Hz).[18] The decreased HOMO–LUMO energy gap (2.72 eV) calculated for **13** compared to **4** (3.03 eV) is in good agreement with its lower stability. Furthermore, at RT, complex **14** isomerizes further by exchange of ligands (H and CH_2) on the Si and Ni centers to give a stable pincer-type nickel(II) hydride complex **16**.[14] Contrary to the related isomerization of **7** to **8**, proceeding via two simultaneous 1,2-migrations of ligands on the Si and Ni atoms (see Figure 5), in the case of **14**, the isomerization proceeds in two steps: i) reductive elimination at the Ni center and formation of a Si–C bond to generate a Si^{IV}-Ni^0 complex **15** with the Si–H moiety interacting with the Ni^0 center, and then ii) oxidative addition of the Si–H moiety to the Ni center to give the final nickel(II)-hydride complex **16**. Although clean NMR spectra of **14** could not be obtained due to the similar kinetics of the two isomerization steps (**14**→**15** and **15**→**16**), careful NMR analysis of the reaction mixture allowed to detect characteristic signals for the Si–H-Ni moiety of **15** in the ^{1}H NMR spectrum ($\delta = -3.48$ ppm, $^2J_{PH} = 4.8$ Hz, $^1J_{SiH} = 104.1$ Hz)[19] and in the ^{29}Si NMR spectrum ($\delta = -15.8$ ppm, $^2J_{SiP} = 28.6$ Hz),[20] strongly supporting the formation of **15** as an intermediate.

In conclusion, a donor-stabilized silylene complex **4** with a Ni^0-based donating ligand (Ni^0→silylene complex) was successfully synthesized. Complex **4**, exhibiting a pyramidalized and nucleophilic Si^{II} center, shows a peculiar chemical behavior due to the cooperative reactivity of the Si and Ni centers. Of particular interest, calculations demonstrate that the orientation of Ni-ligands with respect to the silylene moiety is a crucial factor in determining the role of Ni-fragment (Lewis acid or Lewis base) towards silylene, and a simple 90° rotation of the Si–Ni bond reverses the role of Ni, transforming a classical silylene→Ni^0 complex into an original Ni^0→silylene complex. In addition, calculations also predict that the energy difference between both complex isomers is relatively small and, therefore, such a transformation can occur in solution for models without structural restrictions to prevent the Si–Ni bond rotation and alter their reactivity. More detailed studies on their properties and reactivity are under investigation.

Acknowledgements

We are grateful to the ANR (MMdash and Si-POP), the DGA (RAPID-LIMS, Spherea/CNRS) and Marelli corporation (Marelli next-generation scholarship) and the Spanish AEI (grant PID2020-116861GB-I00) for financial support of this work.

Conflict of Interest

The authors declare no conflict of interest.

Data Availability Statement

The data that support the findings of this study are available from the corresponding author upon reasonable request.

Keywords: Density Functional Calculations · Donor Ligands · Metallacycles · Nickel Complexes · Silylenes

[1] D. F. Shriver, *Acc. Chem. Res.* **1970**, *3*, 231.
[2] A. Amgoune, D. Bourissou, *Chem. Commun.* **2011**, *47*, 859.
[3] J. Bauer, H. Braunschweig, R. D. Dewhurst, *Chem. Rev.* **2012**, *112*, 4329.
[4] a) J. Becica, G. E. Dobereiner, *Org. Biomol. Chem.* **2019**, *17*, 2055; b) R. C. Cammarota, L. J. Clouston, C. C. Lu, *Coord. Chem. Rev.* **2017**, *334*, 100.
[5] a) G. Frenking, M. Sola, S. F. Vyboishchikov, *J. Organomet. Chem.* **2005**, *690*, 6178; b) I. Dalmázio, H. A. Duarte, *J. Chem. Phys.* **2001**, *115*, 1747; c) S. F. Vyboishchikov, G. Frenking, *Chem. Eur. J.* **1998**, *4*, 1428.
[6] D. M. T. Chan, T. B. Murder, *Angew. Chem. Int. Ed. Engl.* **1988**, *27*, 442; *Angew. Chem.* **1988**, *100*, 436.
[7] D. Heitmann, T. Pape, A. Hepp, C. Mück-Lichtenfeld, S. Grimme, F. E. Hahn, *J. Am. Chem. Soc.* **2011**, *133*, 11118.
[8] a) H. Braunschweig, A. Damme, R. D. Dewhurst, F. Hupp, J. O. C. Jimenez-Halla, K. Radacki, *Chem. Commun.* **2012**, *48*, 10410; b) H. Braunschweig, M. A. Celik, R. D. Dewhurst, M. Heid, F. Huppa, S. S. Sen, *Chem. Sci.* **2015**, *6*, 425; c) F. Hupp, M. Ma, F. Kroll, J. O. C. Jimenez-Halla, R. D. Dewhurst, K. Radacki, A. Stasch, C. Jones, H. Braunschweig, *Chem. Eur. J.* **2014**, *20*, 16888.
[9] C. Gendy, A. Mansikkam-ki, J. Valjus, J. Heidebrecht, P. Chuk-Yan Hui, G. M. Bernard, H. M. Tuononen, R. E. Wasylishen, V. K. Michaelis, R. Roesler, *Angew. Chem. Int. Ed.* **2019**, *58*, 154; *Angew. Chem.* **2019**, *131*, 160.
[10] a) T. Cantat, N. Mézailles, L. Ricard, Y. Jean, P. Le Floch, *Angew. Chem. Int. Ed.* **2004**, *43*, 6382; *Angew. Chem.* **2004**, *116*, 6542; b) J. Becker, T. Modl, V. H. Gessner, *Chem. Eur. J.* **2014**, *20*, 11295; c) K.-S. Feichtner, V. H. Gessner, *Chem. Commun.* **2018**, *54*, 6540.
[11] a) C. Watanabe, Y. Inagawa, T. Iwamoto, M. Kira, *Dalton Trans.* **2010**, *39*, 9414; b) T. J. Hadlington, T. Szilvási, M. Driess, *Angew. Chem. Int. Ed.* **2017**, *56*, 7470; *Angew. Chem.* **2017**, *129*, 7578.
[12] G. Knizia, *J. Chem. Theory Comput.* **2013**, *9*, 4834.
[13] D. Gau, T. Kato, N. Saffon-Merceron, A. De Cózar, F. P. Cossío, A. Baceiredo, *Angew. Chem. Int. Ed.* **2010**, *49*, 6585; *Angew. Chem.* **2010**, *122*, 6735.
[14] Deposition Numbers 2149852 (for **4**), 2149853 (for **5**), 2149854 (for **6**), 2149855 (for **8**), 2149856 (for **9** and **10**), 2149857 (for **10**) and 2149858 (for **16**) contain the supplementary crystallographic data for this paper. These data are provided free of charge by the joint Cambridge Crystallographic Data Centre and Fachinformationszentrum Karlsruhe Access Structures service.
[15] For example, Si–Ni bond lengths observed for the complexes **5**, **8**, **10** and **13**: 2.168–2.237 Å.
[16] B. R. Barnett, J. S. Figueroa, *Chem. Commun.* **2016**, *52*, 13829.
[17] a) S. Nlate, E. Herdtweck, R. A. Fischer, *Angew. Chem. Int. Ed. Engl.* **1996**, *35*, 1861; *Angew. Chem.* **1996**, *108*, 1957;

b) R. C. Handford, P. W. Smith, T. D. Tilley, *Organometallics* **2018**, *37*, 4077; c) V. M. Iluc, G. L. Hillhouse, *J. Am. Chem. Soc.* **2010**, *132*, 11890.
[18] a) A. Enachi, M. Freytag, J. Raeder, P. G. Jones, M. D. Walter, *Organometallics* **2020**, *39*, 2470; b) S. Caddick, F. G. N. Cloke, P. B. Hitchcock, A. K. de K. Lewis, *Angew. Chem. Int. Ed.* **2004**, *43*, 5824; *Angew. Chem.* **2004**, *116*, 5948.
[19] a) J. Takaya, N. Iwasawa, *Dalton Trans.* **2011**, *40*, 8814; b) S. Wu, X. Li, Z. Xiong, W. Xu, Y. Lu, H. Sun, *Organometallics* **2013**, *32*, 3227; c) G. Tan, S. Enthaler, S. Inoue, B. Blom, M. Driess, *Angew. Chem. Int. Ed.* **2015**, *54*, 2214; *Angew. Chem.* **2015**, *127*, 2242.
[20] D. Schmidt, J. H. J. Berthel, S. Pietsch, U. Radius, *Angew. Chem. Int. Ed.* **2012**, *51*, 8881; *Angew. Chem.* **2012**, *124*, 9011.

Manuscript received: March 4, 2022
Accepted manuscript online: May 5, 2022
Version of record online: May 25, 2022